VIROLOGY 210, 345–360 (1995)

Intracellular Internalization and Signaling Pathways Triggered by the Large Subunit of HSV-2 Ribonucleotide Reductase (ICP10)

J. C. R. HUNTER,*,† C. C. SMITH,*,‡ DEBASHISH BOSE,*,‡ MICHAEL KULKA,*,‡ R. BRODERICK,‡ and L. AURELIAN,*,†,‡,§,[1]

*Virology/Immunology Laboratories, ‡Department of Pharmacology and Experimental Therapeutics and †Microbiology, University of Maryland School of Medicine, Baltimore, Maryland 21201; and §Department of Biochemistry, The Johns Hopkins Medical Institutions, Baltimore, Maryland 21205

Received November 9, 1994; accepted March 20, 1995

The large subunit of the HSV-2 ribonucleotide reductase (RR) (ICP10) is a chimera consisting of a serine threonine (Ser/Thr) protein kinase domain at the amino terminus and the RR domain at the carboxy terminus. Transformed human cells that constitutively express ICP10 (JHLa1) were stained with anti-*LA-1* antibody (recognizes ICP10 amino acids 13–26) and immunogold-conjugated goat anti-rabbit IgG and were examined by electron microscopy. ICP10-associated gold particles were observed on the cell surface and in structures with ultrastructural characteristics of endocytic vesicles, multivesicular bodies, and lysosomes, consistent with endocytic internalization. ICP10 was also associated with the cytoskeleton fraction of JHLa1 cells and, at least in part, it colocalized with actin filaments. This was evidenced by immunoprecipitation of [^{35}S]methionine-labeled cell fractions and immunofluorescent staining of Triton-treated cells with anti-*LA-1* antibody and phalloidin. Endocytic localization of gold particles was not seen in cells that constitutively express the ICP10 transmembrane (TM)-deleted mutant p139^{TM} (JHL15). p139^{TM} did not associate with the cytoskeleton and was almost entirely localized within the cytoplasm. raf and Erk evidenced decreased mobility consistent with an activated state in JHLa1, but not JHL15, cells, and chloramphenicol acetyl transferase (CAT) expression from a *c-fos/cat* hybrid construct was significantly increased in JHLa1 but not JHL15 cells. The data indicate that effector molecules downstream of *ras* are activated in JHLa1 cells and the ICP10 TM segment plays a critical role in ICP10 intracellular localization and its ability to activate signaling pathways. This behavior is analogous to that of an activated growth factor receptor kinase.

INTRODUCTION

Ribonucleotide reductase (RR) is an essential enzyme for the conversion of ribonucleotides to the corresponding deoxyribonucleotides in eukaryotic and prokaryotic cells, and its activity may represent the rate-limiting step in DNA synthesis and concomitant cell growth (Thelander and Reichard, 1979). Several herpesviruses, including HSV-1, HSV-2, EBV, VZV, pseudorabies virus, and equine herpesvirus types 1 and 3, induce a novel, distinct RR activity (Cohen *et al.*, 1977; Henry *et al.*, 1978; Lankinen *et al.*, 1982; Dutia, 1983; Averett *et al.*, 1983; Davison and Scott, 1987) that may be required for virus growth in nondividing cells (Goldstein and Weller, 1988a,b; Preston *et al.*, 1988; Jacobson *et al.*, 1989). The HSV RR differs from the cellular enzyme in that it is insensitive to dTTP and dATP inhibition and does not have an absolute Mg^{2+} requirement (Langelier and Buttin, 1981). However, like the mammalian and bacterial enzymes, the HSV RR activity is formed by the association of two distinct subunits, the coding regions of which do not overlap. The large subunit (RR1) is a 140-kDa protein, designated ICP6 for HSV-1 and ICP10 for HSV-2. The small subunit (RR2) is a 38-kDa protein encoded by a 1.2-kb mRNA overlapping the 3′ end of the 5.0-kb mRNA that encodes RR1 (Anderson *et al.*, 1981; McLauchlan and Clements, 1983).

Both ICP6 and ICP10 differ from their counterparts in eukaryotic and prokaryotic cells and in other viruses in that they possess a unique N-terminal domain (Nikas *et al.*, 1986; Swain and Galloway, 1986) that has Ser/Thr-specific protein kinase (PK) activity (Chung *et al.*, 1989, 1990; Paradis *et al.*, 1991; Conner *et al.*, 1992). ICP10 also has features of a transmembrane (TM) helical segment at amino acid residues 85–106 (Chung *et al.*, 1990; Luo and Aurelian, 1992; Smith *et al.*, 1994) and SH3 binding motifs (Smith *et al.*, 1994) that might be involved in protein–protein interactions (Koch *et al.*, 1991; Mayer and Baltimore, 1993).

The PK activity of ICP10 is an intrinsic property as evidenced by the following observations: (i) PK activity is associated with a 57-kDa protein expressed by a vector for the ICP10 PK minigene (Chung *et al.*, 1989, 1990), (ii) expression of the ICP10 PK minigene in bacterial expression systems permits the synthesis of an enzymati-

[1] To whom correspondence and reprint requests should be addressed at Virology/Immunology Laboratories, Department of Pharmacology and Experimental Therapeutics and Microbiology, University of Maryland School of Medicine, Baltimore, MD 21201-1192.

0042-6822/95 $12.00

cally active protein (Luo *et al.*, 1991), (iii) ICP10 binds ^{14}C-labeled *p*-fluorosulfonylbenzoyl 5′-adenosine, an ATP analogue, and binding is inhibited by AMP-PNP (Luo and Aurelian, 1992), (iv) kinase activity is retained after ICP10 electrophoresis on a sodium dodecyl sulfate-containing polyacrylamide gel (SDS–PAGE) and renaturation on a nitrocellulose membrane (Luo and Aurelian, 1992), and (v) ICP10 mutants deleted in the PK minigene or in the putative TM segment are PK negative (Luo and Aurelian, 1992). The ICP10 PK minigene causes neoplastic transformation of immortalized cells (Jariwalla *et al.*, 1980; Hayashi *et al.*, 1985; Iwasaka *et al.*, 1985; Ali *et al.*, 1991; Smith *et al.*, 1992, 1994). PK activity is required for transformation as evidenced by the observation that cells which express kinase-negative ICP10 mutants [deleted in the PK domain (p95) or in the TM segment (p139^{TM})] are not transformed (Smith *et al.*, 1994).

Studies of growth factor receptor kinases (GFRs) have shown that in response to their cognate ligands, or when they are constitutively expressed (in transformed cells), the GFRs are activated, resulting in their autophosphorylation and the transphosphorylation of intracellular substrates (Yarden and Ullrich, 1988; Williams, 1989; Schlessinger and Ullrich, 1992) that bind to the receptors and are thereby recruited to the inner surface of the cell membrane (Bar-Sagi *et al.*, 1993a; Panayotou and Waterfield, 1993; Pawson and Schlessinger, 1993). In this way the *ras* proto-oncogene is activated (Buday and Downward, 1993; Chardin *et al.*, 1993; Li *et al.*, 1993). This is followed by the successive phosphorylation and activation of multiple cytoplasmic PKs, including raf-1 (Morrison *et al.*, 1988; App *et al.*, 1991; Wood *et al.*, 1992) and the extracellular signal-regulated kinases (Erks) (De Vries-Smits *et al.*, 1992; Robbins *et al.*, 1992; Wood *et al.*, 1992; Nishida and Gotoh, 1993). Erk2 is involved in the activation of *c-fos* expression (Kortenjann *et al.*, 1994) which has been proposed as a causal event in uncontrolled cell proliferation (Verma, 1986; Miao and Curran, 1994), thereby conceptually linking the transduction of signals from membrane-bound GFRs to the transformation process. A further effect of growth factor stimulation is GFR cytoskeleton binding which may favor signal transduction (Rijken *et al.*, 1991). Given the finding that ICP10 has a functional TM segment (Luo and Aurelian, 1992; Smith *et al.*, 1994), the studies described in this report were designed to examine the internalization and intracellular localization of ICP10 and the signaling pathways with which it is associated.

MATERIALS AND METHODS

Cells

Adenovirus type 5-immortalized human embryo kidney (293) cells were obtained from the American Type Culture Collection and grown in Eagle's modified minimal essential medium (EMEM) with 10% fetal bovine serum (FBS). They express the adenovirus immortalizing E1a protein and have a very low cloning efficiency in agarose (Graham and Smiley, 1977). Lines JHLa1c, JHLa1b, and JHLa1e were independently established from individual G418-selected clones of 293 cells transfected with the expression vector pJW17N (Smith *et al.*, 1994). The vector contains the constitutive simian cytomegalovirus IE94 promoter (CMVIE) regulating the expression of the ICP10 gene and a SV_2neo cassette (Luo and Aurelian, 1992). All three lines evidence anchorage-independent growth (Smith *et al.*, 1994). Lines JHL15a, JHL15b, and JHL15d were independently established from individual G418-selected clones of 293 cells transfected with expression vector pJHL15N. This vector contains the CMVIE promoter regulating expression of an ICP10 TM-deletion mutant and a SV_2neo cassette (Smith *et al.*, 1994). pJHL15N expresses a 139-kDa protein (p139^{TM}) which is PK negative (Luo and Aurelian, 1992). All three JHL15 lines were negative for anchorage-independent growth (Smith *et al.*, 1994). F-9 (mouse embryonal carcinoma) cells lack AP-1 (Angel *et al.*, 1989). They were grown in Dulbecco's modified MEM (DMEM) with 15% FBS.

Plasmids

Plasmid pFC4 that contains the CAT gene under the control of the *c-fos* gene promoter (at positions −404 to +42) was obtained from Dr. I. Verma. Its construction and activation properties were described (Sassone-Corsi *et al.*, 1988). pFC4R contains the *c-fos* promoter of pFC4 in reverse orientation. pTKcat in which the CAT gene is under the control of the HSV-1 thymidine kinase gene promoter (at positions −400 to +60) was constructed in pcatB′ containing the CAT structural gene without eukaryotic promoter sequences (O'Hare and Hayward, 1984). pSV_2cat contains the CAT gene under the control of the simian virus 40 (SV40) early regulatory region. pA_{10}cat contains the SV40 early regulatory region with a deletion in its 72-bp enhancer region (Laimins *et al.*, 1984).

Antibodies

Polyclonal antibody anti-*LA-1* to a peptide located upstream of the ICP10 TM segment (amino acid residues 13–26) and monoclonal antibody (MAb) H3 that recognizes a determinant in the ICP10 RR domain were previously described (Aurelian *et al.*, 1989; Chung *et al.*, 1991). Anti-actin (rabbit polyclonal) antibody A2066 was obtained from Sigma Immunochemicals (St. Louis, MO) and sheep antibody to human lysozyme was obtained from Biodesign International (Kennebunkport, ME). Fluorescein-conjugated goat anti-rabbit IgG was obtained from Organon Teknika (West Chester, PA). Gold-conjugated goat anti-rabbit and donkey anti-sheep IgG were

obtained from Ted Pella (Redding, CA). Anti-Erk antibody (rabbit polyclonal 691) that recognizes both Erk1 and Erk2 and anti-raf-1 antibody (rabbit polyclonal C-12) were obtained from Santa Cruz Biotechnology (Santa Cruz, CA).

Immunofluorescent staining

JHLa1 and JHL15 cells grown on rat tail collagen-coated glass coverslips (Collaborative Biomedical Products, Bedford, MA) were fixed with 3% paraformaldehyde in phosphate-buffered saline (PBS), pH 7.3 (20 min, 23°). In some experiments, fixation was followed by treatment with 0.1% Triton X-100 (in PBS) for 4 min at 23° to identify antigens associated with the cytoskeleton framework (Coomber, 1991). Slides were stained (60 min, 37°) with anti-*LA-1* antibody and fluorescein-conjugated goat anti-IgG as described (Wymer *et al.,* 1989; Smith *et al.,* 1994). Colocalization studies were carried out by simultaneous staining (20 min, 23°) of cells with rhodamine-conjugated phalloidin (Molecular Probes, Inc., Eugene, OR; 6.6 μM in methanol) and anti-*LA-1* antibody with fluorescein-conjugated anti-rabbit IgG (60 min, 37°) as described (Bar-Sagi *et al.,* 1993b). Actin staining was visualized with a rhodamine filter and ICP10 staining with a fluorescein filter. The images were digitized to 24-bit RGB TIFF files and superimposed using Adobe PhotoShop 2.5.1 on a Macintosh Quadra 840AV computer to demonstrate colocalization of ICP10 and actin.

Cryofixation, immunogold staining, and electron microscopy (EM)

JHLa1, JHL15, and 293 cells were trypsinized, washed with PBS by three cycles of centrifugation (2500 *g;* 15 min) and cryofixed (−160°) using a gentleman-jim apparatus (Minnesota Valley Engineering, New Prague, MN). This fixation method was chosen as it is particularly well suited for the study of dynamic processes such as endocytosis (Hayat, 1989). The frozen cell pellet was freeze-substituted with 1% OsO_4 (Ted Pella) in tetrahydofuran (JT Baker, Phillipsburg, NJ) over 72 hr at −160° and rinsed three times in pure tetrahydofuran at room temperature. The pellet was exposed (2 hr; 23°) to 30% plastic [20% Araldite 502, 25% EM bed-812, 3% dibutyl phthalate, 51% dodecenyl succinic anhydride, 1% 2,4,6-tri(dimethylaminoethyl) phenol] (Electron Microscopy Services, Fort Washington, PA) in polypropylene oxide (PO), followed by 70% plastic overnight and fresh 100% plastic in PO for 2 hr. At this time it was transferred to fresh 100% plastic at 65° and allowed to polymerize by incubation for 18 hr as described (Hayat, 1989).

Thin sections (90–100 nm) were placed on 200-mesh nickel grids (Ted Pella), etched with 5% sodium metaperiodate for 15 min to remove surface osmium, washed (four times; 5 min each) in PBS and incubated with 1% bovine serum albumin to prevent nonspecific staining. They were incubated (2 hr; 4°) with the primary antibodies, washed (four times; 5 min each) in PBS and reincubated (1 hr; 4°) with gold-conjugated anti-IgG (Ted Pella). The grids were washed (three times; 5 min each) in PBS, rinsed with distilled water, dried, stained with 5% uranyl acetate in methanol, and rinsed three times in methanol. They were photographed with a Zeiss EM 109 electron microscope. A minimum of 20 cells were examined for each sample. Gold particles in endocytic vesicles, multivesicular bodies (MVB), and lysosomes represent the average of at least 30 and as many as 60 structures each.

Subcellular fractionation, immunoprecipitation, and immunoblotting

The preparation of whole cell extracts was as previously described (Luo and Aurelian, 1992; Smith *et al.,* 1994). Briefly, whole cell extracts were prepared in RIPA buffer [150 m*M* NaCl, 20 m*M* Tris–HCl (pH 7.4), 0.1% SDS, 1% Nonidet P-40 (NP-40), 1% sodium deoxycholate, 1 m*M* phenylmethylsulfonyl fluoride (Sigma), 100 Kallikrein U/ml of aprotinin (Sigma)] and clarified by centrifugation (30 min) at 16,000 *g*. In some experiments, cells labeled (18 hr; 37°) with [^{35}S]methionine (100 μCi/ml, sp act 1120 Ci/m*M;* Dupont NEN Research Products, Boston, MA) in EMEM without methionine and 10% dialyzed FBS were fractionated into soluble (SOL) and cytoskeletal (CSK) components prior to immunoprecipitation. Fractionation was as described by Boss *et al.* (1981). For immunoprecipitation, extracts were incubated (1 hr; 4°) with 10 μl of antibody and 100 μl of protein A–Sepharose CL4B (50% [vol/vol]; Sigma). Beads were washed with cold RIPA buffer and bound proteins were eluted by boiling (3 min) in 100 μl of denaturing solution [150 m*M* Tris hydrochloride (pH 7.0), 5.7% SDS, 14% 2-mercaptoethanol, 17% sucrose, 0.04% bromothymol blue]. Proteins were resolved by SDS–PAGE on 8.5% polyacrylamide gels. Quantitative analysis was done by densitometric scanning of samples equilibrated for protein content using a Molecular Dynamics ImageQuant computing densitometer Model 300B. For immunoblotting, proteins were subjected to SDS–PAGE and electrophoresed onto nitrocellulose membranes. They were incubated with the respective antibodies followed by protein A–peroxidase (Sigma) for 1 hr at room temperature each. Detection was with ECL reagents (Amersham, Arlington Heights, IL) as described (Aurelian *et al.,* 1989; Smith *et al.,* 1994).

raf-1 and Erk assays

Mobility-shift assays were as described (App *et al.,* 1991; Westwick *et al.,* 1994). Briefly, JHLa1 and JHL15 cells were serum starved by growth (24 hr) in DMEM with 0.5% FBS. They were resuspended in denaturing solution and resolved by SDS–PAGE on 7% polyacryl-

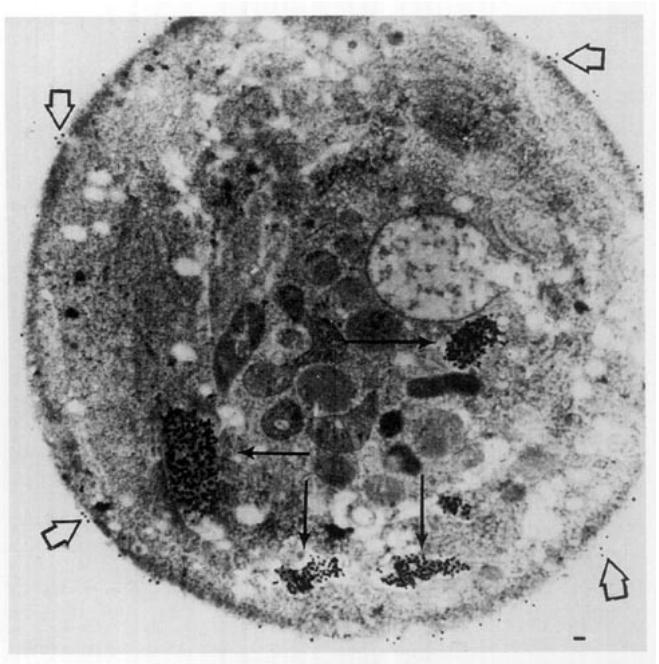

FIG. 1. Electron micrograph of cryofixed JHLa1c cell stained with *anti-LA-1 antibody and 30 nm gold-conjugated anti-rabbit* IgG evidences ICP10 localization on the cell surface (open arrows) and in endocytic vesicles (long closed arrows). Magnification is ×16,000. Bar, 1000 Å.

amide gels for raf-1 assays. Cell extracts were prepared in RIPA buffer and proteins (100 μg) were resolved by SDS–PAGE on 7% polyacrylamide gels for Erk assays. Proteins were electrotransferred onto nitrocellulose membranes and immunoblotted with anti-raf-1 or anti-Erk-1/2 antibodies.

DNA transfection and CAT assays

Cells were plated 24 hr prior to transfection into 25-cm^2 culture flasks (Costar, Cambridge, MA). DNA transfection was performed on a 75–80% confluent monolayer (approximately 10^6 cells) by the calcium phosphate precipitation method which employed a glycerol boost (Wymer *et al.*, 1989). Transfection mixtures contained 3.0 μg of target supercoiled plasmid. Cells were harvested 40–44 hr post-transfection and stored at −20° until assayed. CAT assays were performed and analyzed as described previously (Wymer *et al.*, 1989). Quantitative comparisons were made by measuring the amounts of chloramphenicol acetate product with enzyme levels on the linear part of the curve for product formation versus extract concentration and time.

RESULTS

ICP10 is localized on the cell surface and is internalized in endocytic vesicles

Membrane immunofluorescent staining and cell fractionation experiments have previously shown that ICP10 is associated with the plasma membrane of JHLa1 cells (Luo and Aurelian, 1992; Smith *et al.*, 1994). The present studies sought to determine whether ICP10 can be visualized on the surface of JHLa1 cells by immunogold staining of EM thin sections, which is a more definitive method for intracellular protein localization. We used cell lines JHLa1b, JHLa1c, and JHLa1e that express ICP10 and clone in agarose, and lines JHL15a, JHL15b, and JHL15d, that express the TM-deleted protein p139^{TM} and are negative for anchorage-independent growth (Smith *et al.*, 1994). The cells were stained with anti-*LA-1* antibody and colloidal gold-conjugated goat anti-rabbit IgG and examined by EM. Preimmune rabbit serum was used as a control.

As shown in Fig. 1 for an entire cell, and in a different cell in Fig. 2A for one area of the cell surface (at higher magnification), ICP10 was detected on the surface of JHLa1 cells. A similar distribution of ICP10-associated gold particles was observed for all three JHLa1 lines, but gold particles were not seen on the surface of JHLa1 cells stained with preimmune serum (Fig. 3). p139^{TM} was not seen on the surface of JHL15 cells from all the lines studied in these series (Fig. 4B) and parental 293 cells showed only a small degree of background staining (Fig. 4A). Quantitative estimates based on the number of gold particles on the surface of 8–10 cells in each group are 150 ± 16, 8 ± 1, and 6 ± 2/μm for anti-*LA-1*-stained JHLa1, JHL15, and 293 cells, respectively. Gold particles on the surface of 8 JHLa1 and JHL15 cells stained with preimmune serum are 4 ± 2/μm.

ICP10 is internalized in endocytic vesicles

The endosomal compartment plays a central role in directing the orderly traffic of GFRs and ligand–GFR complexes (Hopkins *et al.*, 1990). After internalization via coated pits, the coated vesicles are rapidly stripped generating smooth endocytic vesicles that are characterized by their size (0.3–0.5 μm) and the high content of receptor or receptor–ligand complexes (Rothman and Schmid, 1986; Gruenberg and Howell, 1989). Molecules destined to be degraded are then transported to late endosomes. These structures, also designated multivesicular bodies, result from the fusion of endocytic vesicles to each other or with a group of tubular cisternae and have a multivesicular appearance. The vesicles are closely associated with the perimeter membrane and often there is a larger (≥0.3-μm diameter) centrally placed vacuole. MVBs are 0.5–1.2 μm in diameter and are often observed in close proximity to lysosomes (Griffiths *et al.*, 1988; Gruenberg *et al.*, 1989; Hopkins *et al.*, 1990).

Our findings for ICP10-associated gold particles in JHLa1 cells are consistent with such an internalization pathway. Gold particles were clustered in surface invagi-

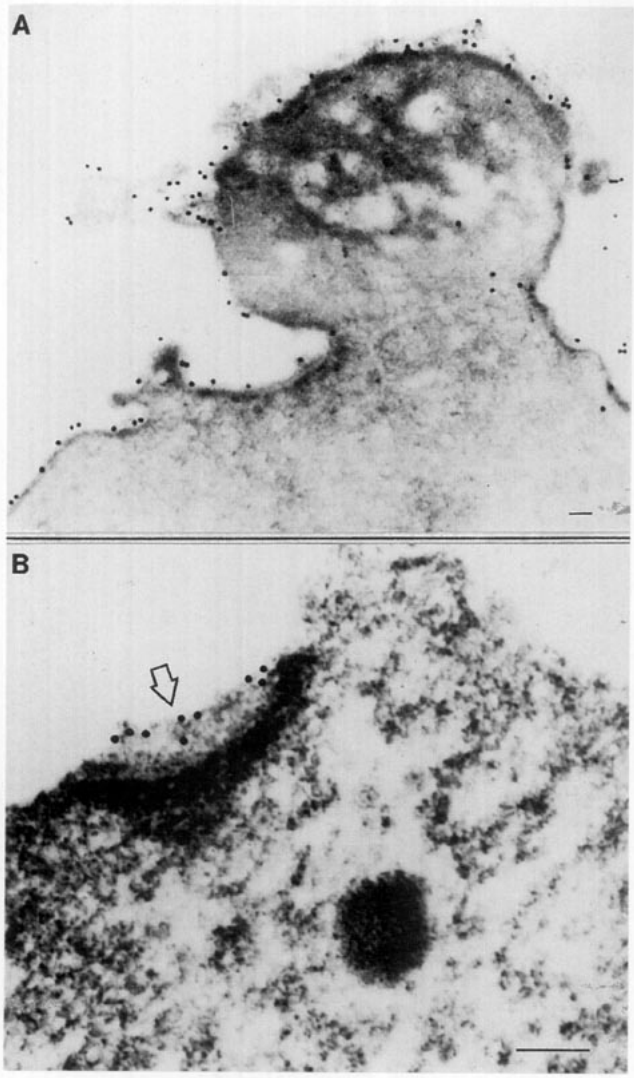

FIG. 2. (A) Magnification of one area of the cell surface of a cryofixed JHLa1b cell stained with anti-*LA-1* antibody and 20 nm gold-conjugated anti-rabbit IgG evidences localization of ICP10 over the cell surface. Magnification is ×45,000. Bar, 1000 Å. (B) Formation of a coated vesicle that contains ICP10 in a JHLa1e cell stained with anti-*LA-1* antibody and 10 nm gold-conjugated goat anti-rabbit IgG. A typical coated pit containing gold particles is shown (open arrow). Magnification is ×125,000. Bar, 1000 Å.

nations (Fig. 2B) that evidenced membrane thickening characteristic of coated pits (Friend and Farquhar, 1967; Korn, 1975; Pryer *et al.*, 1992). The ring-like structure close to the cell membrane shown in Fig. 5A represents a cross-section of a coated pit that has pinched off from the plasma membrane and is transformed into a coated vesicle as evidenced by its thickened membrane (Pearse, 1987). Most of the ICP10-associated gold particles were localized in 0.3–0.5-μm smooth endocytic-like vesicles (Figs. 1 and 5B) and in larger structures that evidenced an uneven ICP10 staining and had the appearance of MVBs. Three types of MVB-like structures are shown in Fig. 6. A cross-section through a 0.8-μm structure that contains two empty vesicles surrounded by gold particles is shown in Fig. 6A. The 1.1-μm structure in Fig. 6B reveals four peripheral vesicles surrounding a large, (0.7-μm) central vacuole. The section is longitudinal and the vesicles' lumens are masked by the cytoplasm presumably due to the angle of the section. The perimeter of the structure consists of a dense accumulation of ICP10-associated gold particles. Figure 6C shows a cross-section through a 1.1-μm structure that has a large empty lumen surrounded by gold particles and containing one dense internal vesicle delineated by gold particles as described for MVB structures involved in the internalization of epidermal growth factor receptor (EGFR) (Felder *et al.*, 1990). The structures in Figs. 6A and 6B are more commonly detected in JHLa1 cells than the structure in Fig. 6C. Colocalization of ICP10 and lysozyme (Fig. 7) suggests that ICP10 is also present within lysosomes. The number of *LA-1*-specific gold particles in the JHLa1 structures is 912 ± 42, 925 ± 207, and 88 ± 17 for endocytic vesicles, MVB, and lysosomes, respectively (Table 1). This is consistent with the conclusion that internalized ICP10 is destined to be degraded (Rothman and Schmid, 1986; Pearse, 1987; Griffiths *et al.*, 1988; Gruenberg and Howell, 1989; Gruenberg *et al.*, 1989; Hopkins *et al.*, 1990; Felder *et al.*, 1990). Most of the gold particles in similarly stained JHL15 cells were randomly distributed throughout the cytoplasm (Fig. 4B; Table 1). This type of intracellular localization cannot be clearly differentiated from background staining. The failure of p139^{TM} to localize in endocytic vesicles is not due to a generalized trafficking defect, since gold-free structures, consistent with endosomes, were observed in JHL15 cells (Fig. 4B).

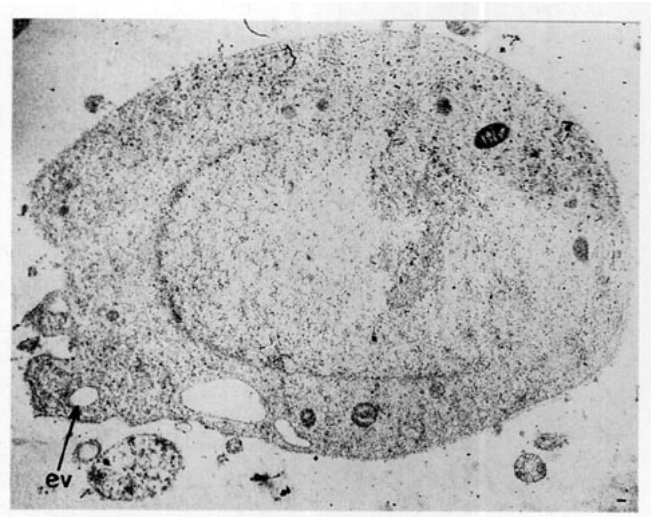

FIG. 3. Electron micrograph of a cryofixed JHLa1c cell stained with preimmune rabbit serum and 20 nm gold-conjugated anti-rabbit IgG does not evidence surface or intracellular staining. Structures consistent with endosomal vesicles (ev) are seen but they do not contain gold particles. Magnification is ×16,000. Bar, 1000 Å.

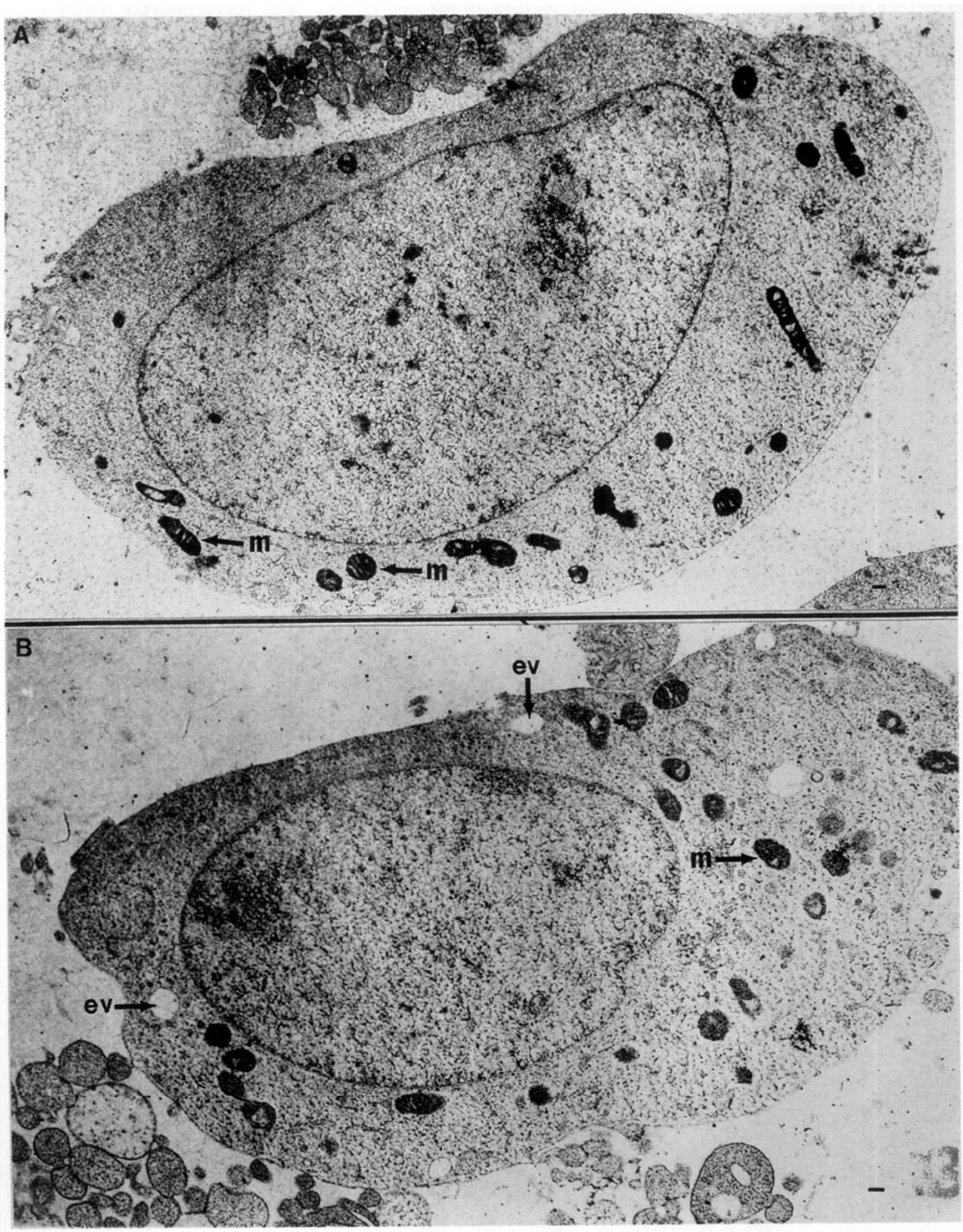

FIG. 4. Electron micrograph of cryofixed 293 (A) and JHL15 (B) cells stained with anti-*LA-1* antibody and 10 nm gold-conjugated goat anti-rabbit IgG. Structures consistent with endosomal vesicles (ev) are seen but they do not contain gold particles (m, mitochondria). Magnification is ×25,000 (A) and ×30,000 (B). Bar, 1000 Å.

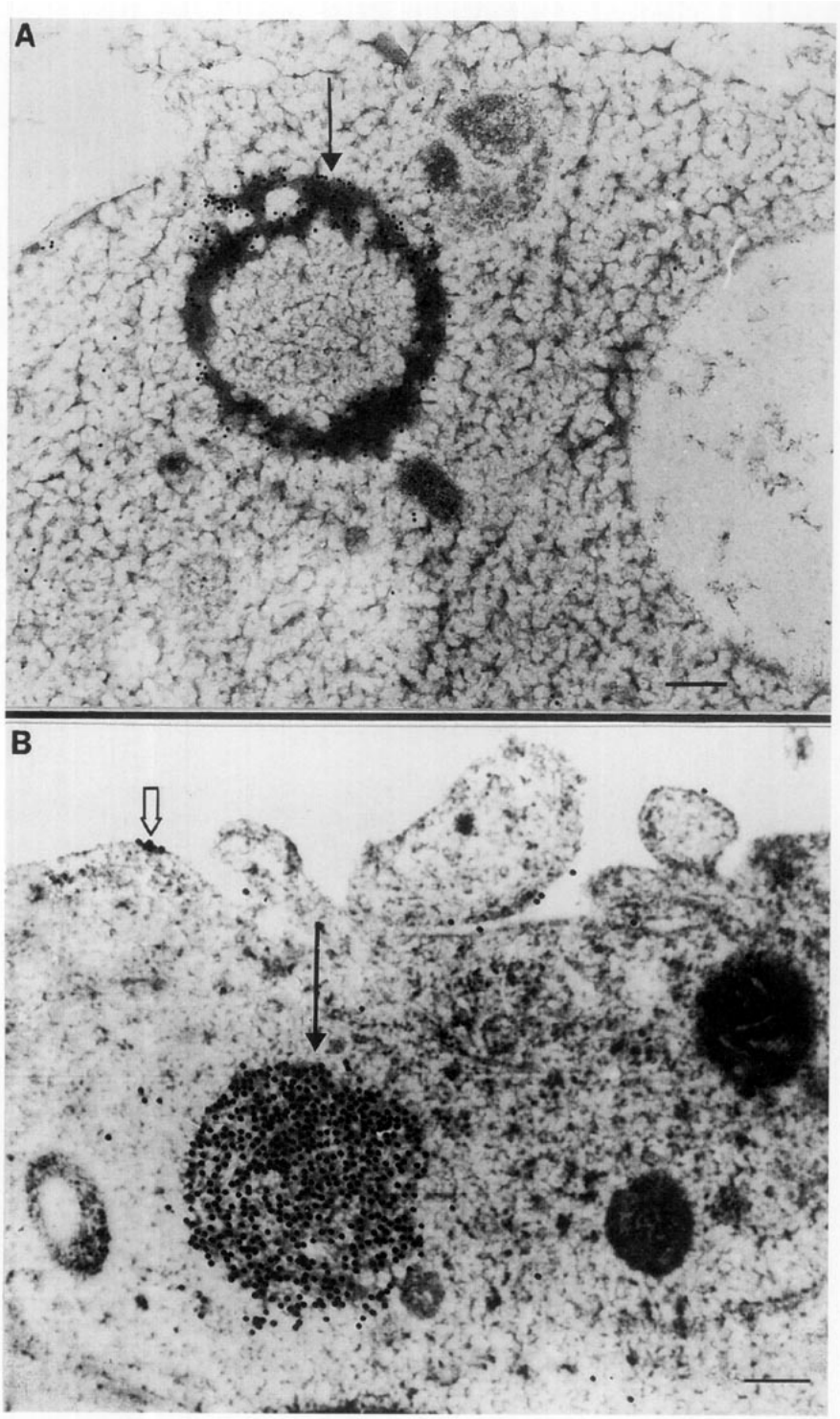

FIG. 5. ICP10 internalization in cryofixed JHLa1 cells stained with anti-*LA-1* antibody and 10 nm gold-conjugated anti-rabbit IgG. (A) Coated vesicle containing ICP10-associated gold particles (arrow). (B) Uncoated endocytic-like vesicle contains large concentration of ICP10 (arrow). Surface-associated gold particles are shown (open arrow). Magnification is ×75,000 (A) and ×80,000 (B). Bar, 1000 Å.

ICP10, but not p139^{TM}, is associated with the cytoskeleton

Previous studies have shown that EGFR is associated with the cytoskeleton, reflecting a high affinity state that favors signal transduction (Rijken *et al.*, 1991; van Bergen en Henegouwen *et al.*, 1992). Two series of experiments were done in order to determine whether ICP10 is also associated with the cytoskeleton. In the first series, extracts of [^{35}S]methionine-labeled JHLa1 and JHL15 cells

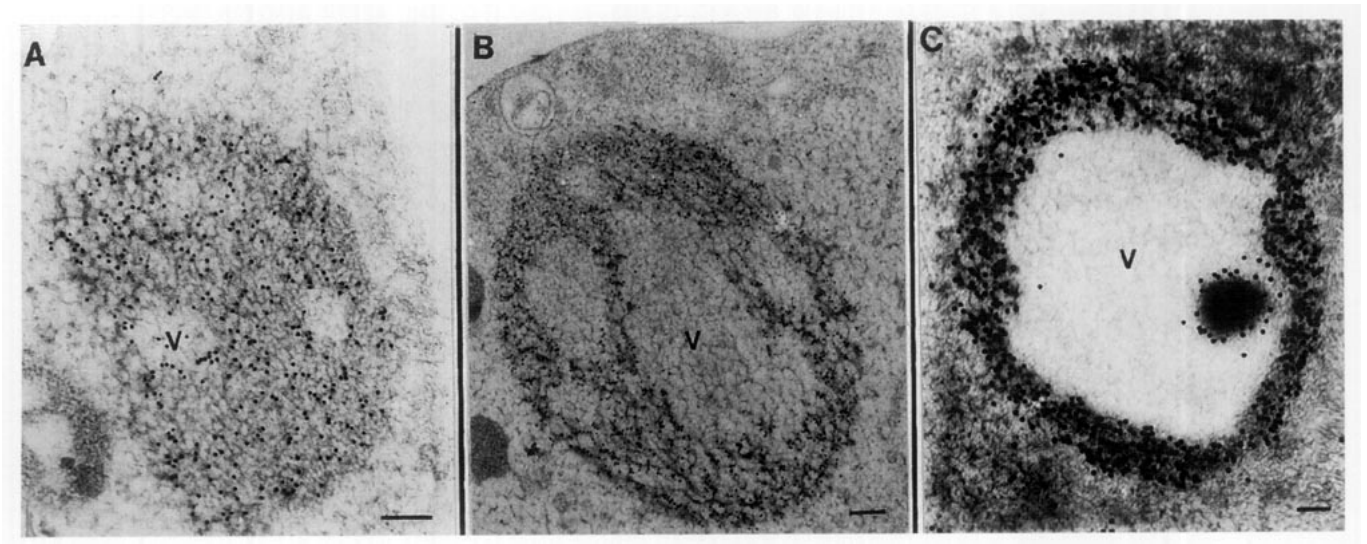

FIG. 6. ICP10 internalization in cryofixed structures consistent with MVBs in JHLa1 cells stained with anti-*LA-1* antibody and gold-conjugated anti-rabbit IgG evidence (A) two vesicles (V) surrounded by gold particles, (B) four peripheral vesicles around a central, large vacuole (V) and delineated by gold particles, or (C) a large, empty lumen (V) surrounded by gold particles and containing a dense internal vesicle also delineated by gold particles. Gold particles in A and B are 20 nm; gold particles in C are 40 nm. Magnification is ×70,000 (A), ×50,000 (B), ×50,000 (C). Bar, 1000 Å.

were fractionated into SOL and CSK fractions and the purity of the fractions was estimated based on the distribution of actin as determined by immunoblotting (Boss *et al.*, 1981; Chung *et al.*, 1989). Actin was recovered in the CSK (Fig. 8, lane 2) but not the SOL (Fig. 8, lane 3) fractions of JHLa1. Densitometric scanning indicated that 95% of the total cellular actin was recovered in the CSK fraction (3321 and 3500 densitometric units for the CSK fraction and the total cell extracts, respectively). However minimal cross-contamination cannot be excluded as evidenced by the nonspecifically recognized bands which are equally distributed in all fractions. Similar results were seen for JHL15 cells. Immunoprecipitation with MAb H3 indicated that ICP10 is present in both the SOL (Fig. 9, lane 3) and CSK (Fig. 9, lane 4) fractions from JHLa1 cells (3666 and 4134 densitometric units for CSK and SOL, respectively), while p139^{TM} was almost exclusively associated with the SOL fraction of JHL15 cells (347 and 3615 densitometric units for CSK and SOL, respectively) (Fig. 9, lane 1). Only 10–15% of the total p139^{TM} expressed in JHL15 cells was associated with the CSK (Fig. 9, lane 2).

In the second series of experiments, the cytoskeleton framework of JHLa1 and JHL15 cells was exposed by fixation with paraformaldehyde followed by Triton X-100 treatment (Bar-Sagi *et al.*, 1993b), and the cells were stained with a 1:100 dilution of anti-*LA-1* antibody in indirect immunofluorescence. Similarly fixed cells that were not treated with Triton and do not reveal the cytoskeleton framework were studied in parallel. Diffuse staining localizing throughout the cytoplasm was observed in both

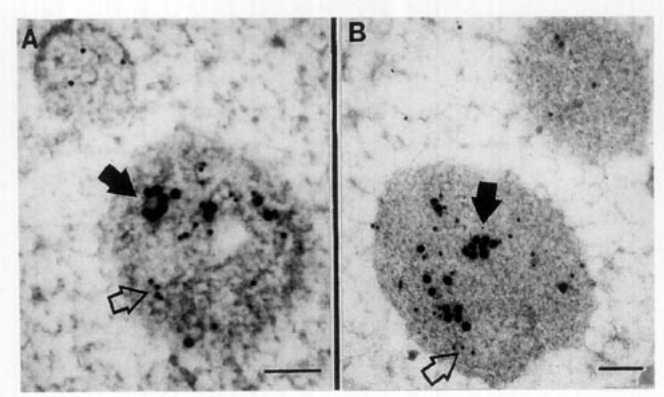

FIG. 7. Colocalization of ICP10 (open arrow) and lysozyme (closed arrow) within lysosomes in cryofixed JHLa1 cells. Cells were stained with both anti-*LA-1* antibody and 10 nm gold-conjugated rabbit IgG and anti-lysozyme antibody and 30 nm gold-conjugated anti-sheep IgG. The numbers of ICP10-related gold particles are lower than in the structures in Figs. 1, 5B, and 6. Magnification is ×95,000 and ×80,000 for A and B, respectively. Bar, 1000 Å.

TABLE 1

Subcellular Distribution of ICP10 in JHLa1 and JHL15 Cells[a]

Intracellular compartment	*Gold particles/μm²*	
	JHLa1	JHL15
Cytoplasm	38 ± 5	101 ± 6
Endocytic vesicle	912 ± 42	NA
MVB	925 ± 207	NA
Lysosomes	88 ± 17	NA
Nucleus	43 ± 9	66 ± 4

[a] Results represent average counts for 20 cells ± SEM. NA, not applicable.

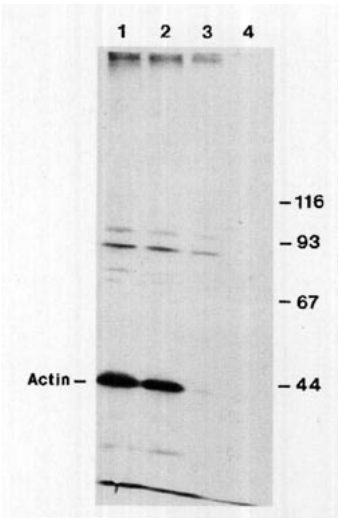

FIG. 8. JHLa1 cells labeled with [^{35}S]methionine for 18 hr were fractionated into SOL and CSK fractions. Total cell extract (lane 1), CSK (lanes 2, 4), and SOL (lane 3) were immunoblotted with anti-actin antibody (lanes 1–3) or preimmune rabbit serum (lane 4). Molecular weight markers are shown on the right. Similar results were obtained with JHL15 cells.

JHLa1 (Figs. 10A and 10C) and JHL15 (Fig. 10B) cells that were not treated with Triton. On the other hand, when cells were Triton treated to expose the cytoskeleton framework, anti-*LA-1* staining was only seen in JHLa1 cells. It was observed in 85–95% of the cells and it localized at the periphery, at cell-to-cell contacts, and in discrete vesicular-like structures distributed at a ratio of 1–2/cell and localizing close to the cell surface (Figs. 10E, 10F, and 10G). Staining also evidenced a capping-like patchy appearance (Fig. 10G) similar to that previously described for EGFR (Kwiatkowska *et al.*, 1991). Triton-treated JHL15 cells did not stain with anti-*LA-1* antibody (Fig. 10H). The failure to detect anti-*LA-1* staining in these cells is not due to improper p139^{TM} expression, nor to the failure of the anti-*LA-1* antibody to recognize this protein, since JHLa1 and JHL15 cells fixed with paraformaldehyde, but untreated with Triton, stained equally well with anti-*LA-1* antibody (Figs. 10A, 10B, and 10C). Preimmune serum was negative (Fig. 10D). Similar results were seen in all the independently established JHLa1 and JHL15 lines studied in these series.

ICP10, but not p139^{TM}, is associated with actin filaments

As actin bundles delineating cell margins were shown to participate in EGFR capping (Kwiatkowska *et al.*, 1991), the question arises whether the anti-*LA-1* staining pattern seen in Triton-treated JHLa1 cells reflects the association of ICP10 with actin filaments. To address this question, JHLa1 cells fixed with paraformaldehyde and treated with Triton were simultaneously stained with a 1:500 dilution of anti-*LA-1* antibody (Fig. 11A) and phalloidin (Fig. 11B) which stains actin filaments (Bar-Sagi *et al.*, 1993b). The dilution of the anti-*LA-1* antibody was five- to sixfold higher than that routinely used (Fig. 10) in order to reduce scatter due to intense staining and allow superimposition of the two staining patterns. Colocalization of ICP10 and actin was evident predominantly at the cell periphery and in some filaments within the cell structure (Fig. 11C), but it was not absolute. Independent localization was also seen for both ICP10 and actin. The discrete *LA-1*-positive vesicles were not seen at this dilution of the anti-*LA-1* antibody and they did not stain with phalloidin. Phalloidin staining patterns in Triton-treated JHL15 cells (data not shown) were similar to those seen in JHLa1 cells. However these cells did not stain with anti-*LA-1* antibody (Fig. 10H).

Mobility shift of raf-1 and Erk in JHLa1 cells

We have previously shown that the levels of activated *ras* (*ras*-GTP) are increased in JHLa1 cells that constitutively express ICP10 compared to JHL15 cells that constitutively express the PK-negative p139^{TM} (Smith *et al.*, 1994). However, effector proteins downstream of *ras* were not studied. Here, we focused on raf-1 and Erk, since several lines of evidence indicate that raf-1 functions in the same signaling pathway as *ras* (Morrison *et al.*, 1988; Wood *et al.*, 1992; Vojtek *et al.*, 1993), and Erk activation by a number of growth factors requires the activity of *ras* (De Vries-Smits *et al.*, 1992; Robbins *et al.*, 1992; Wood *et al.*, 1992; Nishida and Gotoh, 1993).

We used mobility shift assays since previous studies had shown that activated raf-1 and Erk evidence decreased mobility, presumably due to increased phosphorylation (Westwick *et al.*, 1994). Extracts of serum-starved JHLa1 or JHL15 cells (DMEM–0.5% FBS; 24 hr) were immunoblotted with antibodies to raf-1 or Erk 1/2, or with normal rabbit serum. Decreased electrophoretic

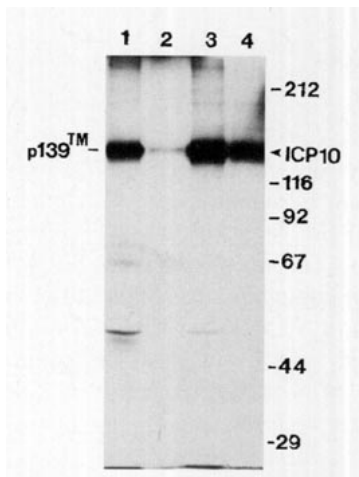

FIG. 9. Immunoprecipitation by MAb H3 from SOL (lane 1) and CSK (lane 2) of JHL15 cells and SOL (lane 3) and CSK (lane 4) of JHLa1 cells studied in Fig. 8. Molecular weight markers are shown on the right.

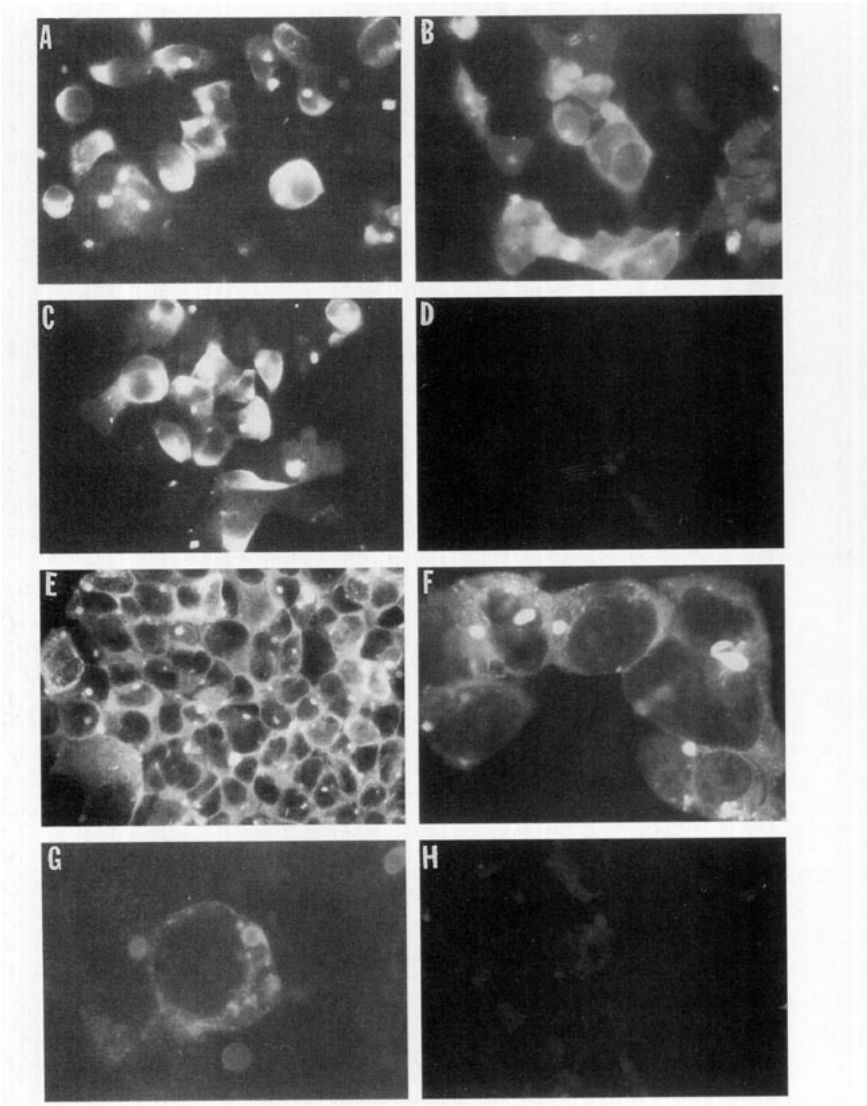

FIG. 10. Indirect immunofluorescent staining with anti-*LA-1* antibody of cells fixed with paraformaldehyde (A–D) or fixed with paraformaldehyde and treated with Triton (E–H). Diffuse cytoplasmic staining is evidenced by JHLa1 cells (A, C) or JHL15 cells (B) stained with anti-*LA-1* antibody but not by JHLa1 (D) or JHL15 (data not shown) cells stained with preimmune serum. Staining of Triton-treated JHLa1 cells with anti-*LA-1* antibody localized at the cell periphery and in vesicular structures (E, F) in a patchy distribution close to the cell surface (F) and it evidenced a polar distribution characteristic of capping (G). Triton-treated JHL15 cells are negative (H).

mobility (active form) was evidenced by raf-1 in JHLa1 cells (Fig. 12A, lane 3) but not in JHL15 cells (Fig. 12B, lane 3). Erk1 and Erk2 also evidenced decreased mobility in JHLa1 (Fig. 12B, lane 3) but not JHL15 (Fig. 12A, lane 2) cells. Normal serum was negative (Figs. 12A and 12B, lanes 1 and 4) and similar results were obtained with all three JHLa1 and JHL15 lines. We interpret these findings to indicate that raf-1 and Erk are activated in cells that constitutively express ICP10 in the absence of exogenously added ligands. They are not activated in cells that express the PK-negative p139^{TM}.

The *c-fos* promoter is activated in JHLa1 cells

Previous studies have shown that GFRs can activate *c-fos* (Curran, 1984; Kruijer *et al.*, 1984), presumably by inducing *ras* signaling pathways. To determine whether ICP10 can cause *c-fos* activation, JHLa1, JHL15, 293, and F-9 cells [lack AP-1 (Angel *et al.*, 1989)] were transfected with a plasmid (pFC4) which contains the CAT gene under the control of the *c-fos* promoter (Sassone-Corsi *et al.*, 1988). Plasmid pTKcat, which uses the HSV-1 thymidine kinase promoter (lacks AP-1 responsive elements), was used as a control. Expression from pFC4 was six- to ninefold higher in JHLa1 (7.2 ± 1.2% conversion) than JHL15 (0.8 ± 0.2% conversion), 293 (1.2 ± 0.5% conversion), or F-9 (0.6 ± 0.1% conversion) cells. Expression from pSV$_2$cat was also increased in JHLa1 cells (45.4 ± 7.2% conversion) compared to JHL15 (10.2 ± 2.8% conversion) or 293 (14.5 ± 4.2% conversion) cells (Table 2). Similar expression levels were observed in three inde-

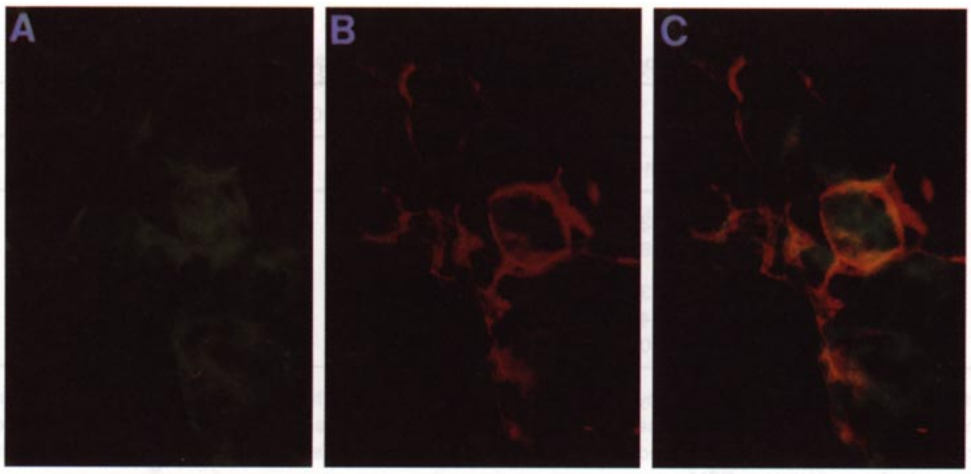

FIG. 11. Immunofluorescent staining of JHLa1b cells with anti-*LA-1* antibody (A) or phalloidin (B). Colocalization of ICP10 and actin as determined by computer superimposition of separately imaged anti-*LA-1* and phalloidin staining is shown in C.

pendent experiments. The percentage conversion in cells transfected with pFC4R (that contains the *c-fos* promoter of pFC4 in the reverse orientation), pTKcat, or pA_{10}-cat was 0.1–1.5% in all cells and similar results were observed for all independently established JHLa1 and JHL15 lines. The increased expression in JHLa1 cells from promoters containing AP-1 responsive elements (pSV_2cat or pFC4) is, at least in part, due to AP-1, since it was not observed in F-9 cells (Table 2).

DISCUSSION

The HSV-1 and HSV-2 RR1 proteins differ from their counterparts in eukaryotic and prokaryotic cells and in other viruses in that they possess a unique amino-terminal region that causes a 50% increase in their molecular weights (Swain and Galloway, 1986; Nikas *et al.*, 1986) and has Ser/Thr specific PK activity (Chung *et al.*, 1989, 1990; Paradis *et al.*, 1991; Conner *et al.*, 1992). Additionally, ICP10 has features of a signal peptide, a TM helical segment followed by a basic residue (Arg^{107}) (Chung *et al.*, 1990; Luo and Aurelian, 1992) that is thought to anchor GFRs to the plasma membrane (Yarden and Ullrich, 1988; Yarden, 1990), and SH3 binding motifs (Smith *et al.*, 1994) that may be involved in protein–protein interactions (Koch *et al.*, 1991). The ICP6 and ICP10 PK domains are only 38% homologous (Nikas *et al.*, 1986), possibly accounting for some of their different properties. Thus, ICP6 PK activity requires NaCl and lower Mn^{2+} and Mg^{2+} concentrations (Paradis *et al.*, 1991) than ICP10 PK (Chung *et al.*, 1989, 1990; Luo *et al.*, 1991; Luo and Aurelian, 1992; Smith *et al.*, 1992), and it is not clear whether it has transphosphorylating activity (Paradis *et al.*, 1991; Conner *et al.*, 1992). The putative TM domain of ICP6 is not followed by basic residues for anchoring to the plasma membrane, and ICP6 lacks a consensus SH3 binding motif (Smith *et al.*, 1994). Unlike ICP10, the ICP6 PK minigene does not cause neoplastic transformation (Camacho and Spear, 1978). The salient features of our findings are the observations that ICP10 is present on the surface of transformed (JHLa1) cells, that it is internalized like activated GFRs, and that it signals through raf-1 and Erk. The following comments seem pertinent with respect to these findings.

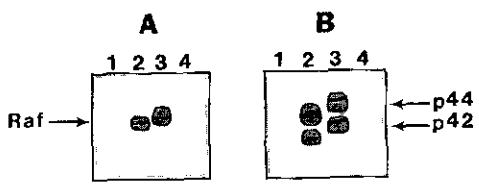

FIG. 12. Mobility shift assays with raf-1 (A) and Erk (B) antibodies. (A) Extracts of JHL15 (lanes 1, 2) or JHLa1 (lanes 3, 4) cells cultured (24 hr) under serum-starved conditions (DMEM–0.5% FBS) were immunoblotted with anti-raf-1 antibody (lanes 2, 3) or preimmune serum (lanes 1, 4) after separation by SDS–PAGE. (B) Duplicates of the same JHL15 (lanes 1, 2) or JHLa1 (lanes 3, 4) cell extracts were immunoblotted with anti-Erk antibody (lanes 2, 3) or preimmune serum (lanes 1, 4).

Immunogold staining with an antibody that recognizes residues upstream of the TM supports previous conclusions that ICP10 is associated with the plasma membrane of JHLa1 cells and the polarity of the association is consistent with a functional TM segment (Luo and Aurelian, 1992; Smith *et al.*, 1994). Indeed, ICP10-related gold particles were seen on the surface of JHLa1, but not JHL15 cells that express the TM-deleted mutant $p139^{TM}$. In JHLa1, but not JHL15, cells gold particles were also seen within structures that are morphologically similar to those involved in the endocytosis of ligand-activated GFRs including coated pits and coated vesicles, endocytic vesicles, MVBs, and lysosomes. Coated pits, defined as indented regions of the membrane which evidence a typical thickening appearance, are involved in

TABLE 2

Activation of the *c-fos* Promoter in Cells That Constitutively Express ICP10[a]

Expt	Construct	% Conversion			
		JHLa1	JHL15	293	F-9
1	pFC4[b]	7.2 ± 1.2	0.8 ± 0.2	1.2 ± 0.5	0.6 ± 0.1
	pTKcat	0.8 ± 0.2	0.5 ± 0.5	0.6 ± 0.2	1.5 ± 0.7
2	pcatB′	0.3 ± 0.3	1.0 ± 0.9	0.5 ± 0.3	0.5 ± 0.5
	pSV_2cat	45.4 ± 7.2	10.2 ± 2.8	14.5 ± 4.2	1.1 ± 0.6
	$pA_{10}cat$	1.0 ± 0.3	1.0 ± 0.5	1.0 ± 0.1	0.8 ± 0.1

[a] Cells were transfected with 3 μg of plasmid DNA by the calcium phosphate method. They were harvested at 44 hr post-transfection and CAT assays were performed as previously described (Wymer *et al.*, 1989). Results are expressed as percentage conversion which is the quantity of chloramphenicol converted to its acetylated form divided by the total quantity of both acetylated and unacetylated chloramphenicol. Results are the average of three independent experiments ± SEM.

[b] Conversion from pFC4R that contains the *c-fos* promoter in reverse orientation was 0.1–0.5% in all lines.

the internalization of membrane proteins, GFRs, and solutes, and sometimes express clathrin (Friend and Farquhar, 1967; Pearse, 1987; Pryer *et al.*, 1992). We observed staining with anti-clathrin antibody in some of the coated pit structures (data not shown) but we cannot exclude the possibility that ICP10 is also internalized through non-clathrin-coated pits. Endosomes are identified by morphological criteria such as their size and the presence of large quantities of internalized proteins. Molecules destined to be degraded in lysosomes are transported from endosomes to MVBs which are larger structures with a complex vesicular or multivesicular appearance and are often observed in the perinuclear region where lysosomes are also found (Griffiths *et al.*, 1988). In addition to ultrastructural criteria, subcellular fractionation, kinetics of internalization, recycling, and degradation, and acidification properties have been used to differentiate MVBs from endosomes (Fuchs *et al.*, 1989). However, exact distinction between the various structures is difficult because of the lack of *bona fide* endosomal markers (Gruenberg *et al.*, 1989). In our studies, ICP10-containing structures other than lysosomes were defined strictly on the basis of ultrastructural criteria. The presence of ICP10 within lysosomes, on the other hand, was unequivocally established by its colocalization with lysozyme as determined in double-staining experiments with anti-*LA-1* and anti-lysozyme antibody.

The failure of $p139^{TM}$ to localize in structures characteristic of the endocytic pathway is not due to a generalized trafficking defect. Indeed, JHL15 cells contained gold-free structures consistent with endocytic vesicles, and immunogold staining with transferrin antibody indicated that it is internalized equally well in both JHLa1 and JHL15 cells (data not shown). It is also not due to poor expression of $p139^{TM}$ or to the use of an inappropriate antibody since: (i) JHLa1 and JHL15 cells stained equally well with anti-*LA-1* antibody and (ii) $p139^{TM}$ was precipitated as well as ICP10 by MAb H3 that is specific for a different ICP10 determinant (in the RR domain). By both of these methods, $p139^{TM}$ was almost exclusively associated with the soluble fraction, an association that is difficult to document in immunogold staining due to losses resulting from the fixation procedure and to the difficulty in differentiating it from nonspecific staining.

In the absence of a putative ligand, final conclusions as to the nature and kinetics of ICP10 internalization are premature. We believe that ICP10 is internalized by the endocytic pathway, since: (i) it was primarily detected in endocytic vesicles and MVBs, (ii) it colocalized with lysozyme, and (iii) the number of ICP10-associated gold particles in lysosomes was lower than that in endocytic vesicles, supporting the conclusion that it undergoes lysosomal degradation. In this context it is significant to point out that oncogenic modification of GFRs is generally related to escape from ligand-bound downregulation by lysosomal degradation (Yarden, 1990). However, ligand-bound EGFR was shown to cause transformation which was attributed to high levels of EGFR expression (Velu *et al.*, 1987). The conclusion that ICP10 undergoes lysosomal degradation is consistent with such an interpretation.

Several immunocytochemical and biochemical data indicate that when cells are exposed to a ligand, the GFRs become linked to the cytoskeleton thereby possibly improving the efficiency of the transformation-associated signaling cascade (Rijken *et al.*, 1991; van Bergen en Henegouwen *et al.*, 1992). Upon EGF binding, actin bundles that delineate cell margins are translocated and aggregate on one side of the cell, a phenomenon described as capping (Kwiatkowska *et al.*, 1991). Our findings for ICP10 are similar. Thus, ICP10, but not $p139^{TM}$, was associated with the cytoskeleton as determined both by immunoprecipitation and by immunofluorescent staining of Triton-treated cells. Staining with both anti-

LA-1 antibody and phalloidin indicated that, at least in part, ICP10 colocalizes with actin filaments. The functional significance of the ICP10 association with the cytoskeleton must await the results of further studies with antibodies to cytoskeleton components, or to adaptor proteins (viz. Ash/Grb-2) potentially required for ICP10 association with the cytoskeleton (Matuoka *et al.,* 1993). Antibodies to downstream effectors (viz. *rac*) that are required for ligand-induced cytoarchitecture reorganization (Ridley *et al.,* 1992), may also help clarify the functional significance of this interaction. As SH3 motifs have been identified in several cytoskeletal proteins and were implicated in the regulation of the cytoskeletal interaction with signaling molecules (Bar-Sagi *et al.,* 1993b), it may be possible that the interaction between ICP10 and the cytoskeleton involves the SH3 binding motifs within ICP10. Implicit in this interpretation is the assumption that the failure of p139^{TM} to associate with the cytoskeleton is due to modification of SH3-binding motifs by secondary/tertiary structure alterations resulting from TM deletion. Alternatively, cytoskeleton association requires an intact PK activity. Similar studies with JHL9 cells which express a PK-deleted ICP10 mutant that has retained its TM segment (Luo and Aurelian, 1992; Smith *et al.,* 1994) should help define the role of the ICP10 PK activity, if any, in cytoskeleton association.

The GTP-bound (active) form of *ras* transduces the GFR-initiated signal to downstream effector proteins including raf-1 (Morrison *et al.,* 1988; Wood *et al.,* 1992; Vojtek *et al.,* 1993) and Erk (De Vries-Smits *et al.,* 1992; Robbins *et al.,* 1992; Wood *et al.,* 1992; Nishida and Gotoh, 1993). The activated state of these proteins is reflected by a decrease in electrophoretic mobility following hyperphosphorylation and is detected in immunoblotting assays with specific antibodies (App *et al.,* 1991; Westwick *et al.,* 1994). *c-fos* activation is a downstream consequence of the activation of Erk (Kortenjann *et al.,* 1994). We have previously shown that *ras* is activated in JHLa1, but not in JHL15, cells, an activation that correlates with transforming potential (Smith *et al.,* 1994). The present studies with antibodies to raf-1 and Erk revealed apparently higher molecular weight species in JHLa1 than in JHL15 cells, suggesting that they are activated, and consistent with the interpretation that they function as downstream effectors of the *ras* pathway, also in JHLa1 cells. The *c-fos* promoter was also activated in JHLa1 cells, presumably related to increased levels of AP-1 factors. However, our results do not go so far as to demonstrate that raf-1 and/or Erk are directly involved in *c-fos* activation, nor do they demonstrate a causal role for constitutive *c-fos* expression in ICP10-induced transformation. Additionally, our studies do not provide direct evidence of a cause and effect relationship between *ras* activation and the activation of raf-1, Erk, and *c-fos.* The finding that *ras* (Smith *et al.,* 1994), as well as raf-1, Erk, and *c-fos,* is not activated in JHL15 cells is consistent with the interpretation that the signal initiated by the ICP10 PK activity involves *ras* and the PK cascade that includes raf-1 and Erk and culminates in *c-fos* activation. However, multiple pathways are capable of stimulating raf-1 activity (Morrison *et al.,* 1988; Kizaka-Kondoh *et al.,* 1992) and the contribution of other factors that may be activated by ICP10, but not p139^{TM}, cannot be excluded. Finally, the exact role of *c-fos* activation in cell replication/transformation remains unclear.

Previous studies suggested that the ICP10 PK minigene may have evolved from a cellular gene that was inserted into the polypeptide coding region of an ancestral HSV RR1 (Smith *et al.,* 1991). Implicit in this interpretation is the assumption that by participating in the viral life cycle, the cellular gene provided a functional advantage that justified its conservation. Therefore a critical question is the role of the ICP10 PK minigene in the virus life cycle. Murine studies indicated that ICP6-deleted mutants replicate poorly at the site of inoculation (ocular) and in neurons they evidence decreased ability to establish latency, and they reactivate less well than the wild-type virus, presumably reflecting decreased growth in infected hosts (Jacobson *et al.,* 1989; Brandt *et al.,* 1991; Idowu *et al.,* 1992). Mutants in RR2 are also less neurovirulent (Cameron *et al.,* 1988), suggesting that RR activity is required, at least for neurovirulence. However, the role of the PK relative to the RR domain in latency establishment/reactivation is unclear. The finding that ICP10 has AP-1 elements and can be activated by *c-jun* (Wymer *et al.,* 1989, 1992) suggests that it may respond to virus-reactivating stimuli that induce transient and/or low levels of AP-1 early in the reactivation process (Valyi-Nagy *et al.,* 1991). Since ICP10 behaves as an activated GFR, its expression may function to initiate signaling pathways that further increase AP-1 levels thereby activating viral/cellular genes required for the resumption of virus replication. Ultimately ICP10 also provides the RR activity that is required for viral DNA synthesis in neurons. Consistent with the interpretation that ICP10 PK is also involved in signaling pathways in HSV-2-infected cells, previous studies have shown that it is associated with the plasma membrane and the cytoskeleton fraction from virus-infected cells (Chung *et al.,* 1989). Because ICP6 may lack transphosphorylating activity and plasma membrane localization as well as an AP-1 element and a consensus SH3 motif, its PK activity may not be similarly involved in the reactivation of HSV-1 from latency. Indeed, other viral proteins have been implicated in HSV-1 reactivation (Cai *et al.,* 1993; Whitley *et al.,* 1993), suggesting that different viral functions may be involved, depending on the virus type. Implicit in the interpretation that ICP6 PK is not required for latency reactivation is the assumption that it has another function in the virus life cycle that remains to be established.

Further conclusions as to the respective roles of the ICP10 PK and RR domains in the virus life cycle must await the results of ongoing studies with HSV-2 mutants deleted in the PK and/or RR domains of ICP10. Comparison between these viruses and viruses carrying the wild-type RR1 in infection and latency may provide important information on the role of the PK minigene and its signaling pathway in the virus life cycle.

ACKNOWLEDGMENTS

These studies were supported by Public Health Service Grant CA39691 from the National Cancer Institute. We thank Deniece Garnett for help with the figures. Dr. Louis Marzella provided invaluable assistance with the interpretation of the EM data and many helpful suggestions.

REFERENCES

Ali, M. A., McWeeney, D., Milosavljevic, A., Jurka, J., and Jariwalla, R. J. (1991). Enhanced malignant transformation induced by expression of a distinct protein domain of ribonucleotide reductase large subunit from herpes simplex virus type 2. *Proc. Natl. Acad. Sci. USA* **88,** 8257–8261.

Anderson, K. P., Frink, R. J., Devi, G. B., Gaylord, B. H., and Wagner, E. K. (1981). Detailed characterization of the mRNA mapping in the *Hin*dIII fragment K region of the herpes simplex virus type 1 genome. *J. Virol.* **37,** 1011–1027.

Angel, P., Smeal, T., Meek, J., and Karin, M. (1989). Jun and v-jun contain multiple regions that participate in transcriptional activation in an interdependent manner. *New Biologist* **1,** 35–43.

App, H., Hazan, R., Zilberstein, A., Ullrich, A., Schlessinger, J., and Rapp, U. (1991). Epidermal growth factor (EGF) stimulates association and kinase activity of Raf-1 with the EGF receptor. *Mol. Cell. Biol.* **11,** 913–919.

Aurelian, L., Terzano, P., Smith, C. C., Chung, T. C., Shamsuddin, A., Costa, S., and Orlandi, C. (1989). Amino terminal epitope of herpes simplex virus type 2 ICP10 protein as a molecular diagnostic marker for cervical intraepithelial neoplasia. *In* "Cancer Cells," Vol. 7, "Molecular Diagnostics of Human Cancer," pp. 187–191. Cold Spring Harbor Laboratory, Cold Spring Harbor, NY.

Averett, D. R., Lubbers, C., Elion, G. B., and Spector, T. (1983). Ribonucleotide reductase induced by herpes simplex type 1 virus. Characterization of a distinct enzyme. *J. Biol. Chem.* **258,** 9831.

Bar-Sagi, D., Margolis, B., and Schlessinger, J. (1993a). Guanine-nucleotide-releasing factor hSos1 binds to Grb2 and links receptor tyrosine kinases to Ras signalling. *Nature (London)* **363,** 85–88.

Bar-Sagi, D., Rotin, D., Batzer, A., Mandiyan, V., and Schlessinger, J. (1993b). SH3 domains direct cellular localization of signalling molecules. *Cell* **74,** 83–91.

Boss, M. A., Dreyfuss, G., and Baltimore, D. (1981). Localization of the Abelson murine leukemia virus protein in a detergent-insoluble subcellular matrix: Architecture of the protein. *J. Virol.* **40,** 472–481.

Brandt, C. R., Kintner, R. L., Pumfrey, A. M., Visali, R. J., and Grau, D. (1991). The herpes simplex virus ribonucleotide reductase is required for ocular virulence. *J. Gen. Virol.* **72,** 2043–2049.

Buday, L., and Downward, J. (1993). Epidermal growth factor regulates p21ras through the formation of a complex of receptor, Grb2 adapter protein, and Sos nucleotide exchange factor. *Cell* **73,** 611–620.

Cai, W., Astor, T. L., Liptak, L. M., Cho, C., Coen, D. M., and Schaffer, P. A. (1993). The herpes simplex virus type I regulatory protein ICP0 enhances virus replication during acute infection and reactivation from latency. *J. Virol.* **67,** 7501–7512.

Camacho, A., and Spear, G. (1978). Transformation of hamster embryo fibroblasts by a specific fragment of the herpes simplex virus genome. *Cell* **15,** 993–1002.

Cameron, J. M., McDougall, I., Marsden, H. S., Preston, V. G., Ryan, D. M., and Subak-Sharpe, J. H. (1988). Ribonucleotide reductase encoded by herpes simplex virus is a determinant of the pathogenicity of the virus in mice and a valid antiviral target. *J. Gen. Virol.* **69,** 2607–2612.

Chardin, P., Camonis, J. H., Gale, N. W., VanAelst, L., Schlessinger, J., Wigler, M., and Bar-Sagi, D. (1993). Human Sos1: A guanine nucleotide exchange factor for *Ras* that binds to Grb2. *Science* **260,** 1338–1343.

Chung, T. D., Wymer, J. P., Kulka, M., Smith, C. C., and Aurelian, L. (1989). Protein kinase activity associated with the large subunit of the herpes simplex virus type 2 ribonucleotide reductase (ICP10). *J. Virol.* **63,** 3389–3398.

Chung, T. D., Wymer, J. P., Kulka, M., Smith, C. C., and Aurelian, L. (1990). Myristylation and polylysine-mediated activation of the protein kinase domain of the large subunit of herpes simplex virus type 2 ribonucleotide reductase (ICP10). *Virology* **179,** 168–178.

Chung, T. D., Luo, J. H., Wymer, J. P., Smith, C. C., and Aurelian, L. (1991). Leucine repeats in the large subunit of herpes simplex virus type 2 (HSV-2) ribonucleotide reductase (ICP10) are involved in RR activity and subunit complex formation. *J. Gen. Virol.* **72,** 1139–1144.

Cohen, J. C., Henry, B. E., Randall, C. C., and O'Callaghan, D. J. (1977). Ribonucleotide reductase activity in hydroxyurea-resistant herpesvirus replication. *Proc. Soc. Exp. Biol. Med.* **155,** 395–399.

Conner, J., Cooper, J., Furlong, J., and Clements, J. B. (1992). An autophosphorylating but not trans-phosphorylating activity is associated with the unique N-terminus of the herpes simplex virus type 1 ribonucleotide reductase large subunit. *J. Virol.* **66,** 7511–7516.

Coomber, B. L. (1991). Cytoskeleton in TFG-β and bFGF-modulated endothelial monolayer repair. *Exp. Cell Res.* **194,** 42–47.

Curran, T. (1984). Induction of c-fos gene and protein by growth factors precedes activation of c-myc. *Nature (London)* **312,** 716–720.

Davison, A. J., and Scott, J. E. (1987). The complete DNA sequence of varicella-zoster virus. *J. Gen. Virol.* **67,** 1759–1816.

De Vries-Smits, A. M. M., Burgering, B. M. T., Leevers, S. J., Marshall, C. J., and Bos, J. L. (1992). Involvement of $p21^{ras}$ in activation of extracellular signal-regulated kinase 2. *Nature (London)* **357,** 602–604.

Dutia, B. M. (1983). Ribonucleotide reductase induced by herpes simplex virus has a virus-specified constituent. *J. Gen. Virol.* **64,** 513–521.

Felder, S., Miller, K., Moehren, G., Ullrich, A., Schlessinger, J., and Hopkins, C. R. (1990). Kinase activity controls the sorting of the epidermal growth factor receptor within the multivesicular body. *Cell* **61,** 623–634.

Friend, D. S., and Farquhar, M. G. (1967). Functions of coated vesicles during protein absorption in the rat vas deferens. *J. Cell Biol.* **35,** 357–376.

Fuchs, R., Schmid, S., and Mellman, I. (1989). A possible role for sodium potassium-ATPase in regulating ATP-dependent endosome acidification. *Proc. Natl. Acad. Sci. USA* **86,** 539–543.

Goldstein, D. J., and Weller, S. K. (1988a). The HSV-1-induced ribonucleotide reductase activity is dispensable for virus growth and DNA synthesis: Isolation and characterization of an ICP6 *lacZ* insertion mutant. *J. Virol.* **62,** 195–205.

Goldstein, D. J., and Weller, S. K. (1988b). Factor(s) present in herpes simplex virus type 1-infected cells can compensate for the loss of the large subunit of the viral ribonucleotide reductase: Characterization of an ICP6 deletion mutant. *Virology* **166,** 41–51.

Graham, F. L., and Smiley, J. (1977). Characteristics of a human cell line transformed by DNA from human adenovirus type 5. *J. Gen. Virol.* **36,** 59–72.

Griffiths, G., Hoflack, B., Simons, K., Mellman, I., and Kornfeld, S. (1988).

The mannose-6-phosphate receptor and the biogenesis of lysosomes. *Cell* **52,** 329–341.

Gruenberg, J., and Howell, K. E. (1989). Membrane traffic in endocytosis: Insights from cell-free assays. *Annu. Rev. Cell Biol.* **5,** 453–481.

Gruenberg, J., Griffiths, G., and Howell, K. E. (1989). Characterization of the early endosome and putative endocytic carrier vesicles *in vivo* and with an assay of vesicle fusion *in vitro*. *J. Cell Biol.* **108,** 1301–1316.

Hayashi, Y., Iwasaka, T., Smith, C. C., Aurelian, L., Lewis, G. K., and Ts'o, P. O. P. (1985). Multistep transformation by defined fragments of herpes simplex virus type 2 DNA: Oncogenic region and its gene product. *Proc. Natl. Acad. Sci. USA* **82,** 8493–8497.

Hayat, M. A. (1989). Principles and techniques of electron microscopy. *In* "Biological Applications," pp. 377–406. CRC Press, Boca Raton, FL.

Henry, B. E., Glaser, R., Hewetson, J., and O'Callaghan, D. J. (1978). Expression of altered ribonucleotide reductase activity associated with the replication of Epstein–Barr virus. *Virology* **89,** 262–271.

Hopkins, C. R., Gibson, A., Sahipman, M., and Miller, K. (1990). Movement of internalized ligand–receptor complexes along a continuous endosomal reticulum. *Nature (London)* **346,** 335–339.

Idowu, A. D., Fraser-Smith, E. B., Poffenberger, K. L., and Herman, R. C. (1992). Deletion of the herpes simplex virus type 1 ribonucleotide reductase gene alters virulence and latency *in vivo*. *Antiviral Res.* **17,** 145–156.

Iwasaka, T., Smith, C., Aurelian, L., and Ts'o, P. O. P. (1985). The cervical tumor-associated antigen (ICP-10/AG-4) is encoded by the transforming region of the genome of herpes simplex virus type 2. *Jpn. J. Cancer Res.* **76,** 946–958.

Jacobson, J. G., Leib, D. A., Goldstein, D. J., Bogard, C. L., Schaffer, P. A., Weller, S. K., and Coen, D. M. (1989). A herpes simplex virus ribonucleotide reductase deletion mutant is defective for productive acute and reactivateable latent infections of mice and for replication in mouse cells. *Virology* **173,** 276–283.

Jariwalla, R. J., Aurelian, L., and Ts'o, P. O. P. (1980). Tumorigenic transformation induced by a specific fragment of DNA from herpes simplex virus type 2. *Proc. Natl. Acad. Sci. USA* **77,** 2279–2283.

Kizaka-Kondoh, S., Sato, K., Tamura, K., Nojima, H., and Okayama, H. (1992). Raf-1 protein kinase is an integral component of the oncogenic signal cascade shared by epidermal growth factor and platelet-derived growth factor. *Mol. Cell. Biol.* **12,** 5078–5086.

Koch, C. A., Anderson, D., Moran, M. F., Ellis, C., and Pawson, T. (1991). SH2 and SH3 domains: Elements that control interactions of cytoplasmic signaling proteins. *Science* **252,** 668–674.

Korn, E. D. (1975). Biochemistry of endocytosis. *In* "MTP International Review of Science," Vol. 2 (C. F. Fox, Ed.) pp. 1–26. Butterworths, London.

Kortenjann, M., Thomae, O., and Shaw, P. (1994). Inhibition of v-*raf*-dependent c-*fos* expression and transformation by a kinase-defective mutant of the mitogen-activated protein kinase Erk2. *Mol. Cell. Biol.* **14,** 4815–4824.

Kruijer, W., Cooper, J. A., Hunter, T., and Verma, M. (1984). Platelet-derived growth factor induces rapid but transient expression of the c-fos gene and protein. *Nature (London)* **312,** 711–720.

Kwiatkowska, K., Khrebtukova, I. A., Gudkova, D. A., Pinaev, G. P., and Sobota, A. (1991). Actin-binding proteins involved in the capping of epidermal growth factor receptors in A431 cells. *Exp. Cell Res.* **196,** 255–263.

Laimins, L. A., Gruss, P., Pozzatti, R., and Khoury, G. (1984). Characterization of enhancer elements in the long terminal repeat of moloney murine sarcoma virus. *J. Virol.* **49,** 183–189.

Langelier, Y., and Buttin, G. (1981). Characterization of ribonucleotide reductase induction in BHK-21/C13 Syrian hamster cell line upon infection by herpes simplex (HSV). *J. Gen. Virol.* **57,** 21–31.

Lankinen, H., Grasiund, A., and Thelander, L. (1982). Induction of a new ribonucleotide reductase after infection of mouse L cells with pseudorabies virus. *J. Virol.* **41,** 893–900.

Li, N., Batzer, A., Daly, R., Yajnik, V., Skolnik, E., Chardin, P., Bar-Sagi, D., Margolis, B., and Schlessinger, J. (1993). Guanine-nucleotide-releasing factor hSos1 binds to Grb2 and links receptor tyrosine kinases to Ras signalling. *Nature (London)* **363,** 85–88.

Luo, J. H., and Aurelian, L. (1992). The transmembrane helical segment but not the invariant lysine is required for the kinase activity of the large subunit of herpes simplex virus type 2 ribonucleotide reductase (ICP10). *J. Biol. Chem.* **267,** 9645–9653.

Luo, J. H., Smith, C. C., Kulka, M., and Aurelian, L. (1991). A truncated protein kinase domain of the large subunit of herpes simplex virus type 2 ribonucleotide reductase (ICP10) expressed in *Escherichia coli*. *J. Biol. Chem.* **266,** 20976–20983.

Matuoka, K., Shibasaki, F., Shibata, M., and Takenawa, T. (1993). Ash/Grb-2, a SH2/SH3-containing protein, couples to signalling for mitogenesis and cytoskeletal reorganization by EGF and PDGF. *EMBO J.* **12,** 3467–3473.

Mayer, B. J., and Baltimore, D. (1993). Signalling through SH2 and SH3 domains. *Trends Cell Biol.* **3,** 8–134.

McLauchlan, J., and Clements, J. B. (1983). DNA sequence homology between two co-linear loci on the HSV genome which have different transforming abilities. *EMBO J.* **2,** 1953–1961.

Miao, G. G., and Curran, T. (1994). Cell transformation by c-*fos* requires an extended period of expression and is independent of the cell cycle. *Mol. Cell. Biol.* **14,** 4295–4310.

Morrison, D. K., Kaplan, D. R., Rapp, U., and Roberts, T. M. (1988). Signal transduction from membranes to cytoplasm: Growth factors and membrane-bound oncogene products increase Raf-1 phosphorylation and associated protein kinase activity. *Proc. Natl. Acad. Sci. USA* **85,** 8855–8859.

Nikas, I., McLauchlan, J., Davison, A. J., Taylor, W. R., and Clements, J. B. (1986). Structural features of ribonucleotide reductase. *Proteins:Struct. Funct. Genet.* **1,** 376–384.

Nishida, E., and Gotoh, Y. (1993). The MAP kinase cascade is essential for diverse signal transduction pathways. *Trends Biochem. Sci.* **18,** 128–131.

O'Hare, P., and Hayward, G. S. (1984). Expression of recombinant genes containing herpes simplex virus delayed-early and immediate-early regulatory regions and transactivation by herpes virus infection. *J. Virol.* **52,** 522–531.

Panayotou, G., and Waterfield, M. D. (1993). The assembly of signalling complexes by receptor tyrosine kinases. *Bioessays* **15,** 171–177.

Paradis, H., Gaudreau, P., Massie, B., Lamarche, N., Guilbault, C., Gravel, S., and Langelier, Y. (1991). Affinity purification of active subunit 1 of herpes simplex virus type 1 ribonucleotide reductase exhibiting a protein kinase function. *J. Biol. Chem.* **266,** 9647–9651.

Pawson, Y., and Schlessinger, J. (1993). SH2 and SH3 domains. *Curr. Biol.* **3,** 434–442.

Pearse, B. M. F. (1987). Clathrin and coated vesicles. *EMBO J.* **6,** 2507–2512.

Preston, V. G., Darling, A. A., and McDougall, I. M. (1988). The herpes simplex virus type 1 temperature sensitive mutant ts1222 has a single base pair deletion in the small subunit of ribonucleotide reductase. *Virology* **167,** 458–467.

Pryer, N. K., Wuestehube, L. J., and Schekman, R. (1992). Vesicle-mediated protein sorting. *Annu. Rev. Biochem.* **61,** 471–516.

Ridley, A. J., and Hall, A. (1992). The small GTP-binding protein rho regulates the assembly of focal adhesions and actin stress fibers in response to growth factors. *Cell* **70,** 389–399.

Rijken, P. J., Hage, W. J., van Bergen en Henegouwen, P. M. P., Verkleij, A. J., and Boonstra, J. (1991). Epidermal growth factor induces rapid reorganization of the actin multifilament system in human A431 cells. *J. Cell Sci.* **100,** 491–499.

Robbins, D. J., Cheng, M., Zhen, E., Vanderbilt, C. A., Feig, L. A., and Cobb, M. H. (1992). Evidence for a Ras-dependent extracellular sig-

nal-regulated protein kinase (ERK) cascade. *Proc. Natl. Acad. Sci. USA* **89,** 6924–6928.

Rothman, J. E., and Schmid, S. L. (1986). Enzymatic recycling of clathrin from coated vesicles. *Cell* **46,** 5–9.

Sassone-Corsi, P., Sisson, J. C., and Verma, I. M. (1988). Transcriptional autoregulation of the proto-oncogene *fos. Nature (London)* **334,** 314–319.

Schlessinger, J., and Ullrich, A. (1992). Growth factor signalling by receptor tyrosine kinases. *Neuron* **9,** 383–391.

Smith, C. C., Wymer, J. P., Luo, J., and Aurelian, L. (1991). Genomic sequences homologous to the protein kinase region of the bifunctional herpes simplex virus type 2 protein ICP10. *Virus Genes* **5,** 215–225.

Smith, C. C., Kulka, M., Wymer, J. P., Chung, T. D., and Aurelian, L. (1992). Expression of the large subunit of herpes simplex virus type 2 ribonucleotide reductase (ICP10) is required for virus growth and neoplastic transformation. *J. Gen. Virol.* **73,** 1417–1428.

Smith, C. C., Luo, J. H., Hunter, J. C. R., Ordonez, J. V., and Aurelian, L. (1994). The transmembrane domain of the large subunit of HSV-2 ribonucleotide reductase (ICP10) is required for protein kinase activity and transformation-related signaling pathways that result in *ras* activation. *Virology* **200,** 598–612.

Swain, M., and Galloway, D. A. (1986). Herpes simplex virus specifies two subunits of ribonucleotide reductase encoded by 3′-coterminal transcripts. *J. Virol.* **57,** 802–808.

Thelander, L., and Reichard, P. (1979). Reduction of ribonucleotides. *Annu. Rev. Biochem.* **48,** 133–158.

Valyi-Nagy, T., Deshmane, S., Dillner, A., and Fraser, N. W. (1991). Induction of cellular transcription factors in trigeminal ganglia of mice by corneal scarification, herpes simplex virus type 1 infection, and explantation of trigeminal ganglia. *J. Virol.* **65,** 4142–4152.

van Bergen en Henegouwen, P. M. P., den Hartigh, J. C., Romeyn, P., Verkleij, A. J., and Boonstra, J. (1992). The epidermal growth factor receptor is associated with actin filaments. *Exp. Cell Res.* **199,** 90–97.

Velu, T. J., Beguinot, L., Vass, W. C., Willingham, M. C., Merlino, G. T., Pastan, I., and Lowy, D. R. (1987). Epidermal growth factor-dependent transformation by a human EGF receptor proto-oncogene. *Science* **238,** 1408–1410.

Verma, I. M. (1986). Proto-oncogene *fos:* A multifaceted gene. *Trends Genet.* **2,** 93–96.

Vojtek, A. B., Hollenberg, S. M., and Cooper, J. A. (1993). Mammalian Ras interacts directly with the serine/threonine kinase Raf. *Cell* **74,** 205–214.

Westwick, J. K., Cox, A. D., Der, C. J., Cobb, M. H., Hibi, M., Karin, M., and Brenner, D. A. (1994). Oncogenic Ras activates c-Jun via a separate pathway from the activation of extracellular signal-regulated kinases. *Proc. Natl. Acad. Sci. USA* **91,** 6030–6034.

Whitley, R. J., Kern, E. R., Chatterjee, S., Chou, J., and Roizman, B. (1993). Replication, establishment of latency, and induced reactivation of herpes simplex virus γ_1 34.5 deletion mutants in rodent models. *J. Clin. Invest.* **91,** 2837–2843.

Williams, L. T. (1989). Signal transduction by the platelet-derived growth factor receptor. *Science* **243,** 1564–1570.

Wood, K. W., Sarnecki, C., Roberts, R. M., and Blenis, J. (1992). Ras mediates nerve growth factor receptor modulation of three signal-transducing protein kinases: MAP kinase, Raf-1, and RSK. *Cell* **68,** 1041–1050.

Wymer, J. P., Chung, T. C., Chang, Y. N., Hayward, G. S., and Aurelian, L. (1989). Identification of immediate-early-type cis-response elements in the promoter for the ribonucleotide reductase large subunit form herpes simplex virus type 2. *J. Virol.* **63,** 2773–2784.

Wymer, J. P., Aprhys, C. M. J., Chung, T. D., Feng, C.-P., Kulka, M., and Aurelian, L. (1992). Immediate early and functional AP-1 cis-response elements are involved in the transcriptional regulation of the large subunit of herpes simplex virus type 2 ribonucleotide reductase. *Virus Res.* **23,** 253–270.

Yarden, Y. (1990). Receptor-like oncogenes: Functional analysis through novel experimental approaches. *Mol. Immunol.* **27,** 1319–1324.

Yarden, Y., and Ullrich, A. (1988). Growth factor receptor tyrosine kinases. *Annu. Rev. Biochem.* **57,** 443–478.